



OPEN

Synthesis, in vitro urease inhibitory potential and molecular docking study of benzofuran-based-thiazolidinone analogues

Muhammad Taha¹✉, Fazal Rahim², Hayat Ullah², Abdul Wadood³, Rai Khalid Farooq⁴, Syed Adnan Ali Shah^{5,6}, Muhammad Nawaz⁷ & Zainul Amiruddin Zakaria^{8,9}✉

In continuation of our work on enzyme inhibition, the benzofuran-based-thiazolidinone analogues (1–14) were synthesized, characterized by HREI-MS, ¹H and ¹³CNMR and evaluated for urease inhibition. Compounds 1–14 exhibited a varying degree of urease inhibitory activity with IC₅₀ values between 1.2 ± 0.01 to 23.50 ± 0.70 μM when compared with standard drug thiourea having IC₅₀ value 21.40 ± 0.21 μM. Compound 1, 3, 5 and 8 showed significant inhibitory effects with IC₅₀ values 1.2 ± 0.01, 2.20 ± 0.01, 1.40 ± 0.01 and 2.90 ± 0.01 μM respectively, better than the rest of the series. A structure activity relationship (SAR) of this series has been established based on electronic effects and position of different substituents present on phenyl ring. Molecular docking studies were performed to understand the binding interaction of the compounds.

Benzofuran scaffolds due to its profound chemotherapeutic, physiological properties and their dynamic nature has attracted the attention of chemist during last few years¹. Acting as versatile scaffolds, benzofuran derivatives can be used to synthesize potentially new therapeutic agents². These scaffolds exhibited biological properties such as antimicrobial³, analgesic⁴, anti-hyperglycemic⁵, anti-parasitic⁶, antitumor and kinase inhibitors⁷. Besides these properties benzofuran scaffolds also found application as oxidant⁸, fluorescent sensor⁹, brightening agent, antioxidant and in other field of chemistry and agriculture¹⁰.

Urease is a metalloenzyme contain nickel that is responsible for catalyzing urea hydrolysis to ammonia and carbamate, the latter spontaneously hydrolyzing to carbonic acid and a second molecule of ammonia in an uncatalyzed reaction¹¹. Ammonia molecules thus formed are protonated by water at physiological pH, whereas the carbonic acid dissociates and causes an increase in pH.

¹Department of Clinical Pharmacy, Institute for Research and Medical Consultations (IRMC), Imam Abdulrahman Bin Faisal University, P.O. Box 1982, Dammam 31441, Saudi Arabia. ²Department of Chemistry, Hazara University, Mansehra, Khyber Pakhtunkhwa 21300, Pakistan. ³Department of Biochemistry, Abdul Wali Khan University Mardan, Mardan 23200, Pakistan. ⁴Department of Neuroscience Research, Institute for Research and Medical Consultations (IRMC), Imam Abdulrahman Bin Faisal University, P.O. Box 1982, Dammam 31441, Saudi Arabia. ⁵Atta-ur-Rahman Institute for Natural Product Discovery, Universiti Teknologi MARA, Cawangan Selangor Kampus Puncak Alam, 42300 Bandar Puncak Alam, Selangor D. E., Malaysia. ⁶Faculty of Pharmacy, Universiti Teknologi MARA, Cawangan Selangor Kampus Puncak Alam, 42300 Bandar Puncak Alam, Selangor Darul Ehsan, Malaysia. ⁷Department of Nano-Medicine Research, Institute for Research and Medical Consultations (IRMC), Imam Abdulrahman Bin Faisal University, P.O. Box 1982, Dammam 31441, Saudi Arabia. ⁸Department of Biomedical Science, Faculty of Medicine and Health Sciences, Universiti Putra Malaysia, 43400 Serdang, Selangor, Malaysia. ⁹Halal Institute Research Institute, Universiti Putra Malaysia, 43400 Serdang, Selangor, Malaysia. ✉email: mtaha@iau.edu.sa; zaz@upm.edu.my

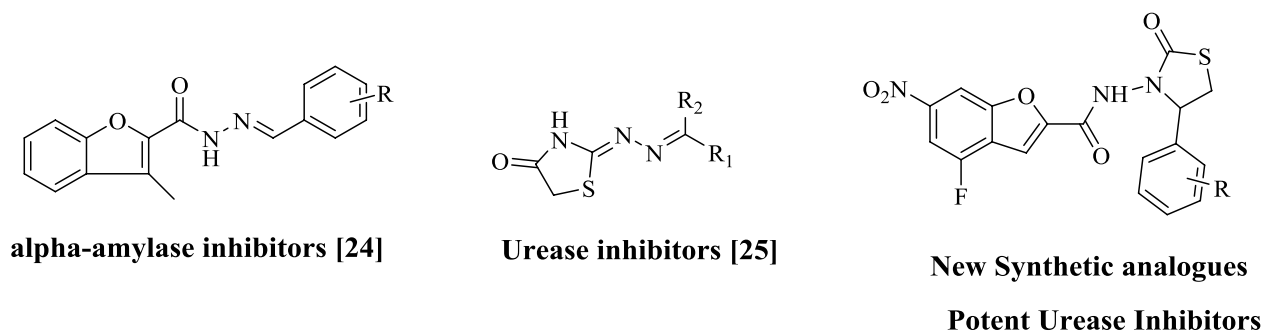
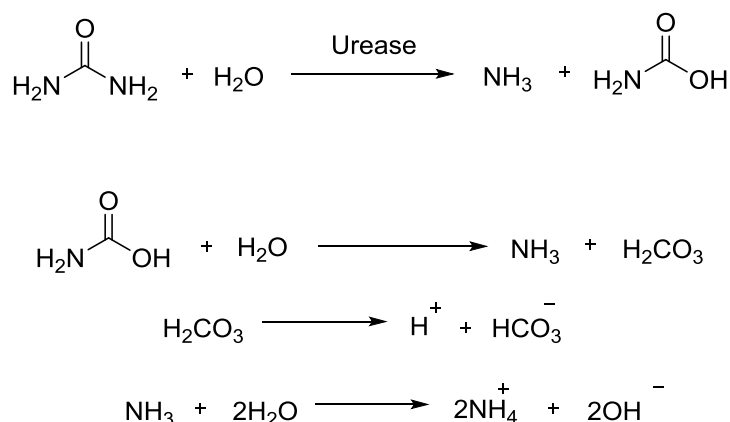


Figure 1. Rational of the current study.



Urease enzyme is involved to function by using urea as nitrogen source^{12,13}. Urease is responsible for the one of the major diseases induced by *Helicobacter pylori*, allowing them to survive inside the stomach at low pH thus play a vital role in peptic and gastric ulcer pathogenesis, apart from cancer too¹². Urease play a key role in the infection stones formation that equally take part in pathogenesis of pyelonephritis, hepatic encephalopathy, urolithiasis, urinary catheter encrustation and hepatic coma¹⁴. Certain secondary complication like ulcer, pus formation and infectious diseases can be treated by inhibiting urease enzyme with help of specific potent inhibitors¹⁵. Previously published urease inhibitors are 2-acylated and sulfonated 4-hydroxycoumarins, bis-indolylmethane thiosemicarbazides and benzimidazole analogues^{16–18}.

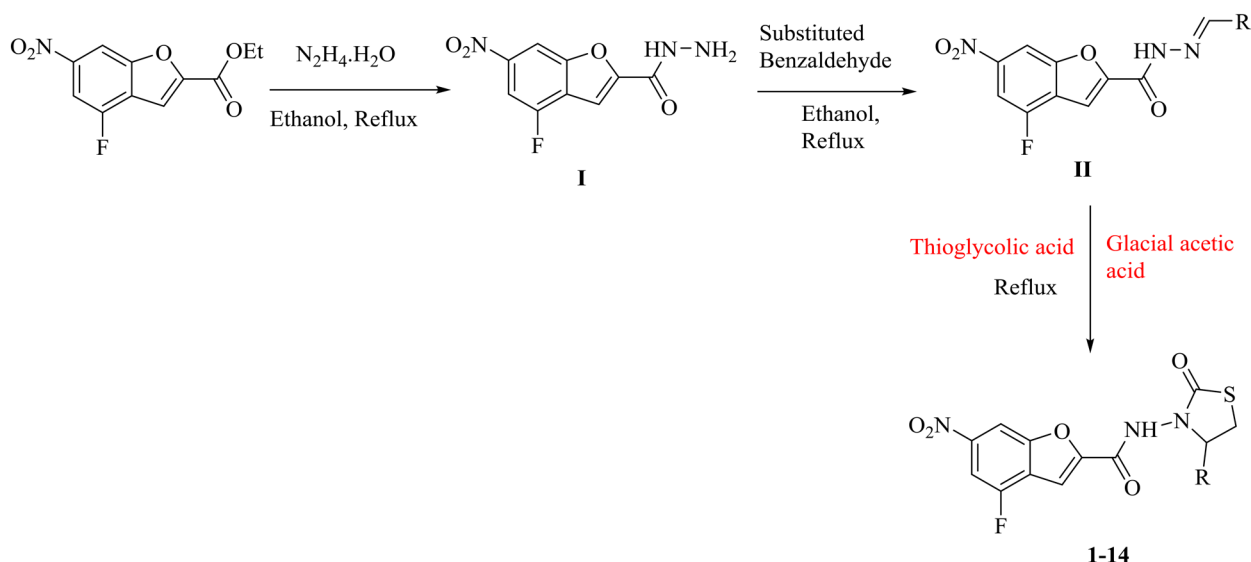
Our research group already has been working on design and synthesis of heterocyclic compounds in search of lead compound since many years and we had some promising outcomes^{19–30}. We had already reported benzofuran hydrazone scaffolds as novel α -amylase inhibitors³¹ (Fig. 1) and thiazolidinone scaffolds as potent urease inhibitors³² but still improvement needed to identify some potential lead compounds for more advance research in future. Keeping in view, here in this study we have design synthesis and biological screening of benzofuran bearing thiazolidinone scaffolds (1–14) as urease inhibitors.

Results and discussion

Chemistry. 4-fluoro-6-nitrobenzofuran-2-carboxylate (1 mmol) was reacted and refluxed with hydrazine hydrate (20 ml) in EtOH (15 ml) to yield 4-fluoro-6-nitrobenzofuran-2-carbohydrazide as intermediated product (I). Then with different substituted benzaldehyde, this intermediate product (I) was reacted and refluxed in EtOH (15 ml) to yield 4-fluoro-6-nitrobenzofuran-2-carbohydrazide as 2nd intermediate product (II). In final step, thioglycolic acid in the presence of few drops of glacial acetic acid was reacted and refluxed with intermediate product (II) to yield desired products of benzofuran bearing thiazolidinone analogues (1–14) (Scheme 1).

In vitro urease inhibitory potential. The synthesized benzofuran bearing thiazolidinone scaffolds (1–14) were evaluated against urease enzyme. Varied degree of potential was exhibited by all scaffolds ranging between 1.2 ± 0.01 to 23.50 ± 0.70 μM comparing with standard drug thiourea ($\text{IC}_{50} = 21.40 \pm 0.21$ μM). Excellent inhibitory potential was exhibited by all synthesized scaffolds. Structure activity relationship (SAR) was established based on different substitution pattern on phenyl ring (Table 1).

Scaffold 1 ($\text{IC}_{50} = 1.2 \pm 0.01$ μM) that has 4-chloro moiety as substituent on phenyl ring was most potent scaffold among the whole series. An excellent potential of this scaffold might be due to the existence of 4-chloro moiety on phenyl ring which is electron withdrawing in nature.



Scheme 1. Synthesis of benzofuran bearing thiazolidinone analogues.

If we compare scaffold **3** ($IC_{50} = 2.2 \pm 0.01 \mu\text{M}$) that has NO_2 moiety at position-2 on phenyl ring with scaffold **6** ($IC_{50} = 5.70 \pm 0.02 \mu\text{M}$) that has NO_2 moiety at position-4 on phenyl ring and scaffold **14** ($IC_{50} = 15.60 \pm 0.50 \mu\text{M}$) that has NO_2 moiety at position-3 on phenyl ring. All these three NO_2 substituted scaffolds showed that the potential difference may be due to the different positions of NO_2 moiety.

If we compare scaffold **2** ($IC_{50} = 6.10 \pm 0.05 \mu\text{M}$) that have hydroxyl at 3- position and methoxy moiety at 4-position on the phenyl ring with scaffold **7** ($IC_{50} = 3.10 \pm 0.01 \mu\text{M}$) that have hydroxyl at 4-position and methoxy group at 3-position on the phenyl ring. The potential difference between these two scaffolds may be due to different positions of hydroxyl and methoxy moiety on the phenyl ring.

Overall it has been concluded that either electron withdrawing groups (EWG) or electron donating groups (EDG) on phenyl ring exhibited good potency but slightly difference in their potency was also mostly affected due to positions of substituents.

Molecular docking. In catalytic pocket of urease enzyme to explore the binding modes of the synthesized scaffolds the Molecular Operating Environment (MOE) package³³ was used to study molecular docking study. With the help of builder tool executed in MOE package, 3D structural coordinates of scaffolds were generated. By using default parameter of MOE, energy of the synthesized scaffolds was minimized, and all 3D coordinates of the scaffolds were protonated. Using PDB code 4UBP, from the online free server protein databank (www.rcsb.org), the crystallographic 3D structure of urease enzyme was retrieved. Next, the structure was added to MOE for protonation, energy to get the stable conformation of protein with the help of default parameter of MOE package. Finally, using the default parameters of MOE package to perform molecular docking studies i.e., Placement: Rescoring 1, Triangle Matcher, Refinement, London dG: Rescoring 2, Forcefield: GBV1/WSA. For each synthesized scaffold, total 10 conformations were allowed to be form. Later, for addition analysis the top ranked conformations were selected.

Docking study. In order to explain the synthesized scaffolds binding pattern, molecular docking studies was conducted in the urease enzyme catalytic pocket (PDB code 4UBP). The urease enzyme catalytic site contains both hydrophobic and hydrophilic site residues (Fig. 2A). The hydrophilic site includes 223, 494, 323, 324, 249, G166, D224, R339 and H315, while hydrophilic site composed of 366, A170, C322, L319 and K169. Furthermore, these two Nickel ions (Ni799 and Ni798) conjointly compete a key role by linking the ligands and key residues. Though, the results of docking showed a well fit sketch of binding in catalytic site and with catalytic residues adopt the most favorable interaction (Fig. 2). Usually, through the binding mode analysis it showed not only that the inhibitory potential of those scaffold was excellent that possess electron withdrawing groups (EWG's) at *para* position, but also with catalytic residues showed favorable interactions. In contrast, among the series in our current study some scaffolds which possess -di- (EWG's) at *para* and *ortho* position that exhibited less potency against urease enzyme. The reason for the decrease in enzyme activity might be that the halides at *para*, *ortho* directing groups most likely prefer to deactivate the benzene ring that result in potency decrease³⁴. Furthermore, the scaffolds among the series that has electron donating groups (EDG's) possess good inhibitory potential against urease enzyme. Though binding mode analysis of most potent scaffold **1** ($1.2 \pm 0.01 \mu\text{M}$) showed the fit well pattern of binding in catalytic site, therefore the scaffold was unable to adopt favorable ionic and other interactions (i.e. hydrophobic, hydrogen bond etc.) with catalytic residues like D363, E223, L365, R339 and with the modified residue KCX220. Furthermore, the two Ni ions (Ni799 & Ni798) accept ionic bond with O13 and S19 of the corresponding scaffold, and additionally improve the potential against urease enzyme (Fig. 2B). High potential of this scaffold might be due to the reason that the attached EWG-1 decreases the

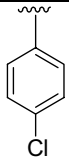
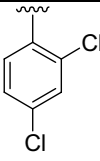
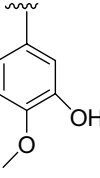
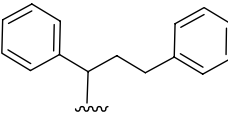
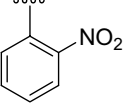
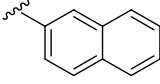
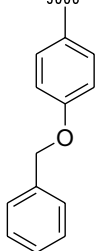
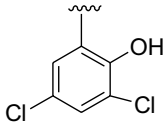
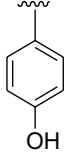
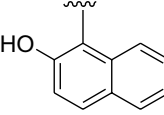
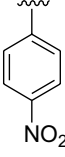
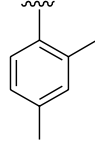
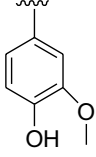
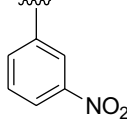
S. no.	R	IC ₅₀ values (μ M)	S. no.	R	IC ₅₀ values (μ M)
1		1.2 ± 0.01	8		2.90 ± 0.01
2		6.10 ± 0.05	9		17.80 ± 0.4
3		2.20 ± 0.01	10		19.60 ± 0.5
4		9.10 ± 0.3	11		11.90 ± 0.4
5		1.40 ± 0.01	12		7.20 ± 0.3
6		5.70 ± 0.02	13		23.50 ± 0.70
7		3.10 ± 0.01	14		15.60 ± 0.50
Thiourea			21.40 ± 0.21		

Table 1. Urease activity and different “R” group of benzofuran bearing thiazolidinone analogues.

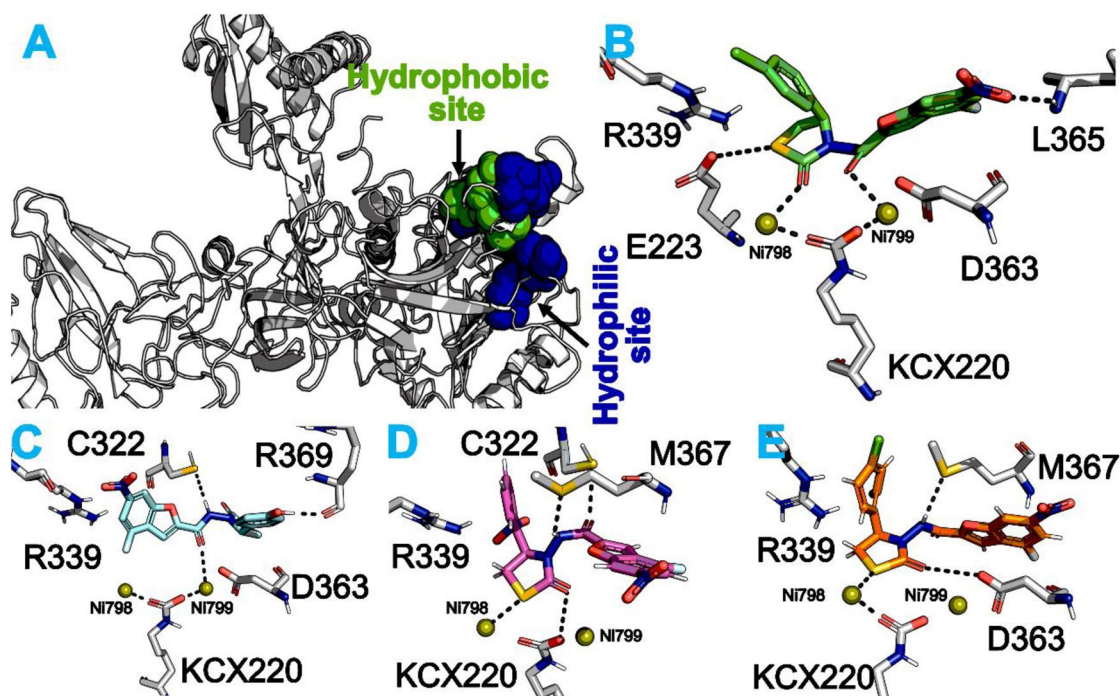


Figure 2. Urease enzyme (PDB code 4UBP) catalytic site binding mode analysis of the most potent scaffolds. (A) Urease enzyme (PDB ID 4UBP) surface representation, hydrophilic and hydrophobic regions are colored to blue and green, furthermore, two Nickel ions (799 and 798) are shown in sphere. In dark black color hydrogen bonding is shown, and π -stacking interactions are shown by both sided arrows. (B) Scaffold-1 mode of interaction (C) Scaffold-5 and (D) Scaffold-3 and (E) Scaffold-8.

π -system electronic density thus making the π -system more electrophilic and hence initiate the partial positive charge on benzene, which make this benzene unable to adopt π -interaction with catalytic residues (R339).

In same manner, the second most potent scaffold 5 that has electron donating group (EDG-OH) among series through binding modes showed the similar binding pattern (Fig. 2C) upon comparison with most potent scaffold 1. In both scaffolds (1 and 5) the difference perceived through binding modes analysis are not only ionic interaction of both Ni ions and modified residues KCX220 but also due to variation in EDG and EWG. Scaffold 5 showed ionic interaction only with single Ni ion while in case of scaffold 1 interaction was with both Ni ions as well as KCX220 residues.

In same manner, the scaffolds 3 and 8 through binding mode analysis showed similar binding mode (Fig. 2D, E). With experimental results the docking results are related well based on key residues with ligands multiple interactions of the urease enzyme. Docking poses of all active scaffolds were computationally reserved the catalytic potentials of urease by firmly binding through hydrogen bonding, strong hydrophobic and polar interactions with key residues.

Conclusion

Benzofuran bearing thiazolidinone scaffolds (1–14) have synthesized in excellent to moderate yield (68–88%). These synthesized scaffolds were evaluated for urease inhibitory potential. All the synthesized scaffolds showed excellent to good inhibitory potential against urease inhibition with IC_{50} value ranging between 1.2 ± 0.01 to 23.50 ± 0.70 μ M as compare to standard thiourea having IC_{50} value 21.40 ± 0.21 μ M. SAR of potent scaffolds was established and were confirmed through molecular docking studies. Among the series, scaffold 1 was found potent urease inhibitor which can act as lead scaffold for further development of drug.

Material and methods

General method for the synthesis of benzofuran-2-carbohydrazide bearing thiazolidinone analogs. 4-fluoro-6-nitrobenzofuran-2-carboxylate was reacted and refluxed with excess of hydrazine hydrate in EtOH to yield 4-fluoro-6-nitrobenzofuran-2-carbohydrazide as intermediated product (I). Then with different substituted benzaldehyde, this intermediate product (I) was reacted and refluxed in EtOH to yield 4-fluoro-6-nitrobenzofuran-2-carbohydrazide as 2nd intermediate product (II). In final step, thioglycolic acid in the presence of glacial acetic acid was reacted and refluxed with intermediate product (II) to yield desired products of benzofuran bearing thiazolidinone analogues (1–14).

N-(4-(4-chlorophenyl)-2-oxothiazolidin-3-yl)-4-fluoro-6-nitrobenzofuran-2-carboxamide (1). Yield: 68%. 1 HNMR (500 MHz, DMSO- d_6): δ 10.05 (s, 1H, NH), 8.81 (s, 1H, Ar), 8.35 (d, $J=2.9$ Hz, 1H, Ar), 7.94 (d, $J=5.15$ Hz, 2H, Ar), 7.87 (s, 1H, Ar), 7.42 (t, $J=0.7, 1.35$ Hz, 2H, Ar), 5.29 (s, 1H, CH), 3.75 (d, $J=1.8$ Hz, 2H,

CH₂). ¹³CNMR (125 MHz, DMSO-*d*₆): δ 165.2, 162.5, 158.5, 157.7, 152.1, 150.2, 141.6, 132.3, 128.6, 128.6, 127.2, 127.2, 124.3, 110.1, 107.4, 104.5, 64.5, 33.4. HREI-MS: m/z calcd for C₁₈H₁₁ClFN₃O₅S [M]⁺ 435.0092, Found 435.0078.

4-Fluoro-N-(4-(3-hydroxy-4-methoxyphenyl)-2-oxothiazolidin-3-yl)-6-nitrobenzofuran-2-carboxamide (2). Yield: 71%. ¹H-NMR (500 MHz, DMSO-*d*₆): δ 10.06 (s, 1H, NH), 8.83 (s, 1H, Ar), 8.36 (t, *J* = 9.45 Hz, 1H, Ar), 7.96 (d, *J* = 7.45 Hz, 2H, Ar), 7.91 (s, 1H, Ar), 7.41 (t, *J* = 5.7, 10.05 Hz, 1H, Ar), 5.13 (s, 1H, CH), 3.87 (d, *J* = 7.55 Hz, 2H, CH₂). ¹³CNMR (125 MHz, DMSO-*d*₆): δ 162.5, 165.2, 158.5, 157.7, 152.1, 150.2, 149.2, 147.2, 136.6, 124.3, 120.0, 114.7, 113.2, 110.1, 107.4, 104.5, 64.5, 55.4, 33.4. HREI-MS: m/z calcd for C₁₉H₁₄FN₃O₇S [M]⁺ 447.0536, Found: 447.0524.

4-Fluoro-6-nitro-N-(4-(2-nitrophenyl)-2-oxothiazolidin-3-yl)benzofuran-2-carboxamide (3). Yield: 78%; ¹H-NMR (500 MHz, DMSO-*d*₆): δ 12.69 (s, 1H, NH), 8.95 (s, 1-H, Ar), 8.39 (d, *J* = 7.55 Hz, 1H, Ar), 8.14 (dd, *J* = 6.50, 6.85 Hz, 1H, Ar), 7.97 (d, *J* = 8.35 Hz, 2H, Ar), 7.86 (t, *J* = 6.25 Hz, 1-H, Ar), 7.73 (t, *J* = 6.45 Hz, 1H, Ar), 5.12 (s, 1-H, CH), 3.86 (d, *J* = 7.57 Hz, 2H, CH₂). ¹³CNMR (125 MHz, DMSO-*d*₆): δ 165.2, 162.5, 158.5, 157.7, 152.1, 150.2, 149.1, 138.4, 135.8, 128.9, 128.2, 125.6, 124.3, 110.1, 107.4, 104.5, 64.5, 33.4. HREI-MS: m/z calcd for C₁₈H₁₁FN₄O₇S [M]⁺ 446.0332, Found 446.0319.

N-(4-(4-(benzyloxy)phenyl)-2-oxothiazolidin-3-yl)-4-fluoro-6-nitrobenzofuran-2-carboxamide (4). Yield: 77%; ¹H-NMR (500 MHz, DMSO-*d*₆): δ 12.22 (s, 1H, NH), 8.84 (d, *J* = 1.8 Hz, 1H, Ar), 8.37 (q, 1H, Ar), 7.97 (d, *J* = 7.6 Hz, 1H, Ar), 7.92 (s, 1H, Ar), 7.71 (d, *J* = 7.2 Hz, 1H, Ar), 7.48 (d, *J* = 6.1 Hz, 1H, Ar), 7.42 (t, *J* = 6.1 Hz, 2H, Ar), 7.36 (d, *J* = 6.05 Hz, 1H, Ar), 7.13 (d, *J* = 7.25 Hz, 2H, Ar), 5.17 (s, 1H, CH), 3.88 (d, *J* = 7.53 Hz, 2H, CH₂). ¹³CNMR (125 MHz, DMSO-*d*₆): δ 165.2, 162.5, 158.5, 157.7, 157.9, 152.1, 150.2, 137.3, 136.1, 129.2, 129.2, 128.9, 128.2, 128.2, 127.4, 127.4, 124.3, 115.4, 115.4, 110.1, 107.4, 104.5, 71.4, 64.5, 33.4. HREI-MS: m/z calcd for C₂₅H₁₈FN₃O₆S [M]⁺ 507.0900, Found 507.0887.

4-Fluoro-N-(4-(4-hydroxyphenyl)-2-oxothiazolidin-3-yl)-6-nitrobenzofuran-2-carboxamide (5). Yield: 88%; ¹H-NMR (500 MHz, DMSO-*d*₆): δ 12.12 (s, 1H, NH), 8.84 (d, *J* = 1.85 Hz, 1H, Ar), 8.41 (s, 1H, Ar), 8.37 (dd, *J* = 2 Hz, 1H, Ar), 7.96 (d, *J* = 7.6 Hz, 1H, Ar), 7.90 (s, 1H, Ar), 7.60 (d, *J* = 7.1 Hz, 2H, Ar), 6.86 (d, *J* = 7.1 Hz, 1H, Ar), 3.87 (d, *J* = 7.50 Hz, 2H, CH₂). ¹³CNMR (125 MHz, DMSO-*d*₆): δ 165.2, 162.5, 158.5, 157.1, 157.9, 152.1, 150.2, 138.4, 129.1, 129.1, 124.3, 117.3, 117.3, 110.1, 107.4, 104.5, 64.5, 33.4. HREI-MS: m/z calcd for C₁₈H₁₂FN₃O₆S [M]⁺ 417.0430, Found 417.0413.

4-Fluoro-6-nitro-N-(4-(4-nitrophenyl)-2-oxothiazolidin-3-yl)benzofuran-2-carboxamide (6). Yield: 70%; ¹H-NMR (500 MHz, DMSO-*d*₆): δ 10.79 (s, 1-H, NH), 8.82 (d, *J* = 1.85 Hz, 1-H, Ar), 8.36 (q, *J* = 1.85 Hz, 2-H, Ar), 7.95 (d, *J* = 7.6 Hz, 2H, Ar), 7.87 (s, 1H, Ar), 5.12 (d, *J* = 7.1 Hz, 1H, Ar), 3.87 (d, *J* = 7.58 Hz, 2H, CH₂). ¹³CNMR (125 MHz, DMSO-*d*₆): δ 165.2, 162.5, 158.5, 157.1, 157.9, 152.1, 150.2, 147.4, 125.3, 125.3, 124.9, 124.9, 124.3, 110.1, 107.4, 104.5, 64.5, 33.4. HREI-MS: m/z calcd for C₁₈H₁₁FN₄O₇S [M]⁺ 446.0332, Found 446.0314.

4-Fluoro-N-(4-(4-hydroxy-3-methoxyphenyl)-2-oxothiazolidin-3-yl)-6-nitrobenzofuran-2-carboxamide (7). Yield: 76%; ¹H-NMR (500 MHz, DMSO-*d*₆): δ 10.79 (s, NH, 1H), 8.82 (d, *J* = 2 Hz, 2-H, Ar), 8.36 (q, *J* = 2.05 Hz, 2-H, Ar), 7.95 (d, *J* = 7.65 Hz, 2H, Ar), 7.87 (s, 1H, Ar), 5.12 (d, *J* = 7.1 Hz, 1H, Ar), 3.98 (s, 3H, OCH₃), 3.87 (d, *J* = 7.48 Hz, 2H, CH₂). ¹³CNMR (125 MHz, DMSO-*d*₆): δ 165.2, 162.5, 158.5, 157.1, 157.9, 152.1, 150.2, 147.9, 147.5, 138.7, 124.3, 120.5, 117.3, 111.6, 110.1, 107.4, 104.5, 64.5, 33.4. HREI-MS: m/z calcd for C₁₉H₁₄FN₃O₇S [M]⁺ 447.0536, Found: 447.0524.

N-(4-(2,4-dichlorophenyl)-2-oxothiazolidin-3-yl)-4-fluoro-6-nitrobenzofuran-2-carboxamide (8). Yield: 73%; ¹H-NMR (500 MHz, DMSO-*d*₆): δ 12.5 (s, 1H, NH), 8.88 (s, 2H, Ar), 8.86 (d, *J* = 1.75 Hz, 2H, Ar), 8.38 (dd, *J* = 1.95 Hz, 2H, Ar), 8.05 (d, *J* = 7.05 Hz, 1H, Ar), 7.97 (d, *J* = 6.4 Hz, 2H, Ar), 7.75 (d, *J* = 1.55 Hz, 1H, Ar), 7.55 (dd, *J* = 1.6, 1 Hz, 1H, Ar), 5.12 (d, *J* = 7.1 Hz, 1H, Ar), 3.87 (d, *J* = 7.57 Hz, 2H, CH₂). ¹³CNMR (125 MHz, DMSO-*d*₆): δ 165.2, 162.5, 158.5, 157.1, 153.2, 151.3, 150.2, 143.4, 135.1, 132.6, 127.8, 124.3, 120.4, 110.1, 107.4, 104.5, 64.5, 33.4. HREI-MS: m/z calcd for C₁₈H₁₀FN₃O₅S [M]⁺ 468.9702, Found: 468.9689.

N-(4-(1,3-diphenylpropyl)-2-oxothiazolidin-3-yl)-4-fluoro-6-nitrobenzofuran-2-carboxamide (9). Yield: 79%; ¹H-NMR (500 MHz, DMSO-*d*₆): δ 11.18 (s, 1H, NH), 8.85 (d, *J* = 1.75 Hz, 3H, Ar), 8.38 (q, *J* = 1.95 Hz, 4H, Ar), 7.99 (d, *J* = 7.55 Hz, 3H, Ar), 7.93 (s, 3H, Ar), 5.12 (d, *J* = 7.1 Hz, 1H, Ar), 3.87 (d, *J* = 7.46 Hz, 2H, CH₂), 1.2 (d, *J* = 3.1 Hz, 5H, aliphatic). ¹³CNMR (125 MHz, DMSO-*d*₆): δ 165.2, 162.5, 158.5, 157.1, 151.3, 150.2, 144.1, 138.4, 131.7, 131.7, 129.9, 129.9, 129.6, 129.6, 128.8, 128.8, 127.6, 126.4, 124.3, 110.1, 107.4, 104.5, 64.5, 41.5, 34.6, 33.9, 33.4. HREI-MS: m/z calcd for C₂₇H₂₂FN₃O₅S [M]⁺ 519.1264, Found: 519.1252.

4-Fluoro-N-(4-(naphthalen-2-yl)-2-oxothiazolidin-3-yl)-6-nitrobenzofuran-2-carboxamide (10). Yield: 74%; ¹H-NMR (500 MHz, DMSO-*d*₆): δ 10.02 (s, 1H, NH), 8.87 (d, *J* = 1.6 Hz, 1H, Ar), 8.82 (d, *J* = 1.96 Hz, 1H, Ar), 8.69 (s, 1H, Ar), 8.39 (dd, *J* = 1.9, 7.55 Hz, 1H, Ar), 8.20 (s, 1H, Ar), 8.06 (m, 3H, Ar), 7.60 (m, 1H, Ar), 5.12 (d, *J* = 7.1 Hz, 1H, Ar), 3.47 (t, *J* = 1.8 Hz, 2H, CH₂). ¹³CNMR (125 MHz, DMSO-*d*₆): δ 165.2, 162.5, 158.5, 157.1, 151.3, 150.2, 136.3, 134.7, 132.3, 129.4, 128.9, 128.4, 128.0, 127.6, 126.8, 125.1, 124.3, 110.1, 107.4, 104.5, 64.5, 33.4. HREI-MS: m/z calcd for C₂₂H₁₄FN₃O₅S [M]⁺ 451.0638, Found: 451.0619.

N-(4-(3,5-dichloro-2-hydroxyphenyl)-2-oxothiazolidin-3-yl)-4-fluoro-6-nitrobenzofuran-2-carboxamide (11). Yield: 75%; ¹H-NMR (500 MHz, DMSO-*d*₆): δ 12.16 (s, 1H, NH), 8.84 (s, 1H, OH), 8.64 (s, 1H, Ar), 8.37 (d, *J* = 7.35 Hz, 1H, Ar), 7.97 (d, *J* = 12 Hz, 1H, Ar), 7.67 (s, 1H, Ar), 5.12 (d, *J* = 7.1 Hz, 1H, Ar), 3.47 (t, *J* = 1.8 Hz, 2H, CH₂). ¹³C-NMR (125 MHz, DMSO-*d*₆): δ 165.2, 162.5, 158.5, 157.1, 151.3, 150.2, 147.8, 135.1, 130.7, 129.4, 127.5, 124.3, 120.0, 110.1, 107.4, 104.5, 64.5, 33.4. HREI-MS: *m/z* calcd for C₁₈H₁₀Cl₂FN₃O₆S [M]⁺ 484.9651, Found 484.9639.

4-Fluoro-*N*-(4-(2-hydroxynaphthalen-1-yl)-2-oxothiazolidin-3-yl)-6-nitrobenzofuran-2-carboxamide (12). Yield: 77%; ¹H-NMR (500 MHz, DMSO-*d*₆): δ 12.99 (s, 1H, OH), 12.51 (s, 1H, NH), 9.56 (t, *J* = 10.1 Hz, 1H, Ar), 8.86 (q, *J* = 9.25 Hz, 1H, Ar), 1H, Ar), 8.39 (dd, *J* = 7.4 Hz, 2H, Ar), 8.0 (m, 4H, Ar), 7.65 (t, *J* = 6.15 Hz, 1H, Ar), 7.44 (t, *J* = 6.2 Hz, 1H, Ar), 7.25 (d, *J* = 7.35 Hz, 1H, Ar), 5.12 (d, *J* = 7.1 Hz, 1H, Ar), 3.47 (t, *J* = 1.9 Hz, 2H, CH₂). ¹³C-NMR (125 MHz, DMSO-*d*₆): δ 165.2, 162.5, 158.5, 157.1, 154.6, 151.3, 150.2, 135.4, 129.7, 129.1, 128.8, 127.7, 125.8, 125.5, 124.3, 120.0, 116.3, 110.1, 107.4, 104.5, 64.5, 33.4. HREI-MS: *m/z* calcd for C₂₂H₁₄FN₃O₆S [M]⁺ 467.0587, Found 467.0578.

N-(4-(2,4-dimethylphenyl)-2-oxothiazolidin-3-yl)-4-fluoro-6-nitrobenzofuran-2-carboxamide (13). Yield: 74%; ¹H-NMR (500 MHz, DMSO-*d*₆): δ 12.23 (s, 1H, NH), 8.84 (d, *J* = 1.85 Hz, 1H, Ar), 8.79 (s, 1H, Ar), 8.38 (q, *J* = 1.95 Hz, 1H, Ar), 7.97 (t, *J* = 7.55 Hz, 2H, Ar), 7.77 (d, *J* = 6.4 Hz, 1H, Ar), 5.12 (d, *J* = 6.2 Hz, 1H, Ar), 3.47 (t, *J* = 3.1 Hz, 2H, CH₂), 2.41 (s, 3H, CH₃), 2.31 (s, 3H, CH₃). ¹³C-NMR (125 MHz, DMSO-*d*₆): δ 165.2, 162.5, 158.5, 157.1, 151.3, 150.2, 139.7, 137.5, 136.1, 131.7, 127.6, 126.5, 124.3, 110.1, 107.4, 104.5, 64.5, 33.4, 22.4, 21.7. HREI-MS: *m/z* calcd for C₂₀H₁₆FN₃O₅S [M]⁺ 429.0794, Found: 429.0782.

4-Fluoro-6-nitro-*N*-(4-(3-nitrophenyl)-2-oxothiazolidin-3-yl)benzofuran-2-carboxamide (14). Yield: 72%; ¹H-NMR (500 MHz, DMSO-*d*₆): δ 12.56 (s, 1H, NH), 8.84 (s, 1H, Ar), 8.61 (s, 1H, Ar), 8.37 (m, 2H, Ar), 8.06 (m, 3H, Ar), 5.12 (d, *J* = 6.2 Hz, 1H, Ar), 3.47 (t, *J* = 3.1 Hz, 2H, CH₂). ¹³C-NMR (125 MHz, DMSO-*d*₆): δ 165.2, 162.5, 158.5, 157.1, 151.3, 150.2, 148.9, 145.4, 135.3, 130.1, 124.3, 122.5, 121.8, 110.1, 107.4, 104.5, 64.5, 33.4. HREI-MS: *m/z* calcd for C₁₈H₁₁FN₄O₇S [M]⁺ 446.0332, Found: 446.0314.

Urease assay protocol. 25 μL of enzyme and 55 μL of buffer was added to 100 mM urea that were incubated with test scaffolds 5 μL (0.5 mM concentration) for 15 min at 30 °C in 96-well plates. Urea concentrations were changed from 2–24 mM to study kinetics. As described by Weatherburn the urease potential was assessed by measuring the ammonia production with using indophenol method³⁵. Concisely, 70 μL of alkali reagent (0.1% active chloride NaOCl and 0.5 w/v NaOH) and 45 μL of reagent phenol (0.005% w/v sodium nitroprusside and 1% w/v phenol) were added to each and every well plate. Using microplate reader (Molecular Device, USA) the increase in absorbance at 630 nm was measured after 50 min. Using 200 μL as final volume the reading was performed as triplicate. With help of SoftMaxPro software (Molecular Device, USA) the results (per min absorbance change) were calculated. At pH 6.8 the entire assay was performed. With the help of 100 – (OD_{test well}/OD_{control}) × 100 the percentage inhibition was calculated. For urease inhibition thiourea was used as standard.

Received: 28 November 2019; Accepted: 8 June 2020

Published online: 30 June 2020

References

- Hayta, S. A. *et al.* Synthesis, antimicrobial activity, pharmacophore analysis of some new 2-(substitutedphenyl/benzyl)-5-[(2-benzofuryl) carboxamido] benzoxazoles. *Eur. J. Med. Chem.* **43**, 2568–2578 (2008).
- Kamal, M., Shakya, A. K. & Jawaid, T. Benzofurans: a new profile of biological activities. *Int. J. Med. Pharm. Sci.* **1**, 1–15 (2011).
- Thévenin, M., Thoret, S., Grellier, P. & Dubois, J. Synthesis of polysubstituted benzofuran derivatives as novel inhibitors of parasitic growth. *Bioorg. Med. Chem.* **21**, 4885–4892 (2013).
- Xie, Y. S. *et al.* Microwave-assisted parallel synthesis of benzofuran-2-carboxamide derivatives bearing anti-inflammatory, analgesic and antipyretic agents. *Tetrahedron Lett.* **55**, 2796–2800 (2014).
- Koca, M. *et al.* Synthesis and antimicrobial activity of some novel derivatives of benzofuran: part 1. Synthesis and antimicrobial activity of (benzofuran-2-yl)(3-phenyl-3-methylcyclobutyl) ketoxime derivatives. *Eur. J. Med. Chem.* **40**, 1351–1358 (2005).
- Cottineau, B., Toto, P., Marot, C., Pipaud, A. & Chenault, J. Synthesis and hypoglycemic evaluation of substituted pyrazole-4-carboxylic acids. *Bioorg. Med. Chem. Lett.* **12**, 2105–2108 (2002).
- Bazin, M. A. *et al.* Synthesis and antiproliferative activity of benzofuran-based analogs of cercosporamide against non-small cell lung cancer cell lines. *Eur. J. Med. Chem.* **69**, 823–832 (2013).
- Oter, O., Ertekin, K., Kirilmis, C., Koca, M. & Ahmedzade, M. Characterization of a newly synthesized fluorescent benzofuran derivative and usage as a selective fiber optic sensor for Fe(III). *Sens. Actuators B Chem.* **122**, 450–456 (2007).
- Karatas, F., Koca, M., Kara, H. & Servi, S. Synthesis and oxidant properties of novel (5-bromobenzofuran-2-yl)(3-methyl-3-methylcyclobutyl) ketonethiosemicarbazone. *Eur. J. Med. Chem.* **41**, 664–669 (2006).
- Habermann, J., Ley, S. V. & Smits, R. Three-step synthesis of an array of substituted benzofurans using polymer-supported reagents. *J. Chem. Soc. Perkin Trans. 1*, 2421–2423 (1999).
- Amtul, Z., Siddiqui, R. A. & Choudhary, M. I. Chemistry and mechanism of urease inhibition. *Curr. Med. Chem.* **9**, 1323–1348 (2002).
- Wilcox, P. E. Chymotrypsinogens-chymotrypsins. *Methods Enzymol.* **19**, 64–108 (1970).
- Benini, S. *et al.* The crystal structure of *Sporosarcina pasteurii* urease in a complex with citrate provides new hints for inhibitor design. *J. Biol. Inorg. Chem.* **18**, 391–399 (2013).
- Schindler, S. Reactivity of copper(I) complexes towards dioxygen. *Eur. J. Inorg. Chem.* **34**, 2311–2326 (2000).
- Wahid, S. *et al.* Atenolol thiourea hybrid as potent urease inhibitors: design, biology-oriented drug synthesis, inhibitory activity screening, and molecular docking studies. *Bioorg. Chem.* **94**, 103359 (2020).
- Rashid, U. *et al.* Synthesis of 2-acylated and sulfonated 4-hydroxycoumarins: in vitro urease inhibition and molecular Docking studies. *Bioorg. Chem.* **66**, 111–116 (2016).

17. Taha, M. *et al.* Bisindolylmethane thiosemicarbazides as potential inhibitors of urease: synthesis and molecular modeling studies. *Bioorg. Med. Chem.* **26**, 152–160 (2018).
18. Zaman, K. *et al.* Synthesis, in vitro urease inhibitory potential and molecular docking study of benzimidazole analogues. *Bioorg. Chem.* **89**, 103024 (2019).
19. Noreen, T. *et al.* Synthesis of alpha amylase inhibitors based on privileged indole scaffold. *Bioorg. Chem.* **72**, 248–255 (2017).
20. Rahim, F. *et al.* Development of bis-thioarbiturates as successful urease inhibitors and their molecular modeling studies. *Chin. Chem. Lett.* **27**, 693–697 (2016).
21. Taha, M. *et al.* Synthesis and biological evaluation of novel *N*-arylidenequinoline-3-carbohydrazides as potent β -glucuronidase inhibitors. *Bioorg. Med. Chem.* **24**, 3696–3704 (2016).
22. Taha, M. *et al.* Biology-oriented drug synthesis (BIODS) of 2-(2-methyl-5-nitro-1Himidazol-1-yl)ethyl aryl ether derivatives, in vitro α -amylase inhibitory activity and in silico studies. *Bioorg. Chem.* **74**, 1–9 (2017).
23. Rahim, F. *et al.* Triazinoindole analogs as potent inhibitors of α -glucosidase: synthesis, biological evaluation and molecular docking studies. *Bioorg. Chem.* **58**, 81–87 (2015).
24. Rahim, F. *et al.* Synthesis, in vitro evaluation and molecular docking studies of thiazole derivatives as new inhibitors of α -glucosidase. *Bioorg. Chem.* **62**, 15–21 (2015).
25. Rahim, F. *et al.* Synthesis, molecular docking, acetylcholinesterase and butyrylcholinesterase inhibitory potential of thiazole analogs as new inhibitors for alzheimer disease. *Bioorg. Chem.* **62**, 106–116 (2015).
26. Rahim, F. *et al.* Isatin based Schiff bases as inhibitors of α -glucosidase: synthesis, characterization, in vitro evaluation and molecular docking studies. *Bioorg. Chem.* **60**, 42–48 (2015).
27. Rahim, F. *et al.* Synthesis and in vitro acetylcholinesterase and butyrylcholinesterase inhibitory potential of hydrazide based schiff bases. *Bioorg. Chem.* **68**, 30–40 (2016).
28. Gollapalli, M. *et al.* Synthesis of bis-indolylmethane sulfonylhydrazides derivatives as potent α -glucosidase inhibitors. *Bioorg. Chem.* **80**, 112–120 (2018).
29. Ullah, H. *et al.* Synthesis, molecular docking study and in vitro thymidine phosphorylase inhibitory potential of oxadiazole derivatives. *Bioorg. Chem.* **78**, 58–67 (2018).
30. Taha, M. *et al.* Synthesis of bis-indolylmethanes as new potential inhibitors of β -glucuronidase and their molecular docking studies. *Eur. J. Med. Chem.* **143**, 1757–1767 (2018).
31. Taha, M. *et al.* Synthesis and in vitro study of benzofuran hydrazone derivatives as novel alpha-amylase inhibitor. *Bioorg. Chem.* **75**, 78–85 (2017).
32. Rahim, F. *et al.* Synthesis of 4-thiazolidinone analogs as potent in vitro anti-urease agents. *Bioorg. Chem.* **63**, 123–131 (2015).
33. Molecular Operating Environment (MOE), 2016.08; Chemical Computing Group Inc., 1010 Sherbrooke St. West, Suite #910, Montreal, QC, Canada, H3A 2R7 (2016).
34. Electron withdrawing group. Illustrated Glossary of Organic Chemistry. UCLA Department of Chemistry (2012).
35. Weatherburn, M. W. Phenol-hypochlorite reaction for determination of ammonia. *Anal. Chem.* **39**, 971 (1967).

Acknowledgements

Authors would like to acknowledge Higher Education Commission of Pakistan for providing a research grant under National Research Program for Universities under Project No. 5721 & 5092.

Author contributions

Conceptualization, M.T. and F.R.; methodology, M.T.; software, A.W.; validation, F.R., H.U. And R.K.F.; formal analysis, M.N.; investigation, S.A.A.S.; resources, M.T.; data curation, M.N. R.K.F. and S.A.A.S.; Writing—Original Draft preparation, M.T. and Z.A.Z.; Writing—Review and Editing, F.R. and Z.A.Z.; visualization, S.A.A.S.; supervision, F.R.; project administration, Z.A.Z. and M.T.; funding acquisition, M.T. and M.N.

Competing interests

The authors declare no competing interests.

Additional information

Supplementary information is available for this paper at <https://doi.org/10.1038/s41598-020-67414-7>.

Correspondence and requests for materials should be addressed to M.T. or Z.A.Z.

Reprints and permissions information is available at www.nature.com/reprints.

Publisher's note Springer Nature remains neutral with regard to jurisdictional claims in published maps and institutional affiliations.



Open Access This article is licensed under a Creative Commons Attribution 4.0 International License, which permits use, sharing, adaptation, distribution and reproduction in any medium or format, as long as you give appropriate credit to the original author(s) and the source, provide a link to the Creative Commons license, and indicate if changes were made. The images or other third party material in this article are included in the article's Creative Commons license, unless indicated otherwise in a credit line to the material. If material is not included in the article's Creative Commons license and your intended use is not permitted by statutory regulation or exceeds the permitted use, you will need to obtain permission directly from the copyright holder. To view a copy of this license, visit <http://creativecommons.org/licenses/by/4.0/>.

© The Author(s) 2020